

AD-A219 669

# Center for Night Vision and Electro-Optics

AMSEL-NV-TR-0090

**ATTENUATION AND MULTIPATH  
EFFECTS ON GROUND VEHICLE  
SIGNATURES FOR 94 GHz SENSORS**

by  
**C. R. Kohler**  
*(C<sup>2</sup>NVEO)*

**H. F. Williams and D. S. Matsumoto**  
*(Rockwell International)*

**FEBRUARY 1990**

Approved for public release; distribution unlimited.



**DTIC**  
**ELECTE**  
MAR 26 1990  
**S E D**

FORT BELVOIR, VIRGINIA 22060-5677

**Destroy this report when it is no longer needed.  
Do not return it to the originator.**

**The citation in this report of trade names of  
commercially available products does not constitute  
official endorsement or approval of the use of such  
products.**

REPORT DOCUMENTATION PAGE				Form Approved OMB No. 0704-0188	
1a. REPORT SECURITY CLASSIFICATION Unclassified		1b. RESTRICTIVE MARKINGS None			
2a. SECURITY CLASSIFICATION AUTHORITY		3. DISTRIBUTION/AVAILABILITY OF REPORT Approved for public release; distribution unlimited.			
2b. DECLASSIFICATION/DOWNGRADING SCHEDULE					
4. PERFORMING ORGANIZATION REPORT NUMBER(S) AMSEL-NV-TR-0090		5. MONITORING ORGANIZATION REPORT NUMBER(S)			
6a. NAME OF PERFORMING ORGANIZATION CECOM, Center for Night Vision and Electro-Optics (C <sup>2</sup> NVEO)		6b. OFFICE SYMBOL (If applicable) AMSEL-RD-NV-V	7a. NAME OF MONITORING ORGANIZATION		
6c. ADDRESS (City, State, and ZIP Code) Director, C <sup>2</sup> NVEO ATTN: AMSEL-RD-NV-SES Fort Belvoir, VA 22060-5677		7b. ADDRESS (City, State, and ZIP Code)			
8a. NAME OF FUNDING/SPONSORING ORGANIZATION ASTAT	8b. OFFICE SYMBOL (If applicable)	9. PROCUREMENT INSTRUMENT IDENTIFICATION NUMBER DAAB07-88-C-F200			
8c. ADDRESS (City, State, and ZIP Code) Assessment of Stationary Target Acquisition Techniques III		10. SOURCE OF FUNDING NUMBERS			
		PROGRAM ELEMENT NO.	PROJECT NO.	TASK NO.	WORK UNIT ACCESSION NO.
11. TITLE (Include Security Classification) Attenuation and Multipath Effects on Ground Vehicle Signatures for 94 GHz Sensors (U)					
12. PERSONAL AUTHOR(S) Charles R. Kohler, H. F. Williams, and D. S. Matsumoto					
13a. TYPE OF REPORT Final	13b. TIME COVERED FROM 2/20/89 TO 3/10/89	14. DATE OF REPORT (Year, Month, Day) February 1990		15. PAGE COUNT 30	
16. SUPPLEMENTARY NOTATION					
17. COSATI CODES			18. SUBJECT TERMS (Continue on reverse if necessary and identify by block number)		
FIELD	GROUP	SUB-GROUP			
19. ABSTRACT (Continue on reverse if necessary and identify by block number)					
<p>The Joint United States-Canadian Obscuration Analysis for Smokes in Snow, also know as <i>Smoke Week XI</i>, was conducted from February 20, 1989, through March 10, 1989, at the Defense Research Establishment in Valcartier, Canada. The purpose of the exercise was to evaluate the performance of a variety of sensors under simulated hostile battlefield environments. These environments include extreme cold, falling snow, and a variety of smoke obscuration over snow-covered terrain. Military vehicles including a Leopard Tank and Armored Personnel Carriers (APCs) were used as targets, as well as a number of corner reflector and dihedral test targets on a fully instrumented test site.</p> <p>This report presents detailed results of the analysis performed on the data collected during <i>Smoke Week XI</i> by the Rockwell Instruments Millimeterwave System (RIMS) operating at 94 GHz. Measurements of snow attenuation, smoke attenuation, snow backscatter, and multipath reflection coefficient were taken at near zero degree grazing angle. The effects of smoke and snow on high range resolution profiles of a Leopard Tank and an M113 APC are also presented. Results are compared to other published results where available. (S) (U)</p>					
20. DISTRIBUTION/AVAILABILITY OF ABSTRACT <input checked="" type="checkbox"/> UNCLASSIFIED/UNLIMITED <input checked="" type="checkbox"/> SAME AS REPORT <input type="checkbox"/> DTIC USERS			21. ABSTRACT SECURITY CLASSIFICATION Unclassified		
22a. NAME OF RESPONSIBLE INDIVIDUAL Charles R. Kohler			22b. TELEPHONE (Include Area Code) 703-664-3498	22c. Office Symbol AMSEL-RD-NV-V	

TABLE OF CONTENTS

	Page
<b>SECTION I INTRODUCTION .....</b>	<b>1</b>
RIMS Description.....	2
Test Objectives .....	3
<b>SECTION II TEST DATA .....</b>	<b>5</b>
Attenuation in Snow .....	5
Attenuation in Smoke .....	6
Snow Backscatter .....	8
Multipath Measurements .....	11
<b>SECTION III SNOW AND SMOKE EFFECTS ON TARGETS.....</b>	<b>14</b>
<b>SECTION IV SUMMARY .....</b>	<b>20</b>
<b>REFERENCES .....</b>	<b>21</b>
<b>APPENDIX TYPICAL SMOKE CONCENTRATION</b>	
<b>LENGTHS (g/m<sup>2</sup>).....</b>	<b>A-1</b>

**FIGURES**

1	Data Acquisition System Description.....	2
2	Plan View of Range (Smoke Week XI).....	4
3	Photographs of Test Site .....	4
4	Attenuation in Snow Results .....	5
5	Cluttermap of Test Area (500-1,200m), HH Polarization, 3/4/89 .....	9
6	Cluttermap of Test Area, HH Polarization .....	9
7	Snow Backscatter Results, HH Polarization.....	10
8	<i>Multipath in Snow Results</i> .....	11
9	Effect of Smoke and Snow on Range Profiles .....	14
10	Expected Target Detection Performance in Clutter as Polarization Varies .....	15
11	Leopard Tank, Clear, 280° Aspect.....	17
12	Leopard Tank, Falling Snow Plus Brass/Fog Oil Smoke, 280° Aspect .....	17
13	Leopard Tank with Aluminum Smoke, 280° Aspect.....	18
14	M113 APC, Clear, 0° Aspect.....	18
15	M113 APC with Graphite Smoke, 0° Aspect .....	19

## TABLES

1	Estimated (Two-Way) Attenuation in Smoke Per Unit Concentration Length.....	7
2	Polarimetric Clutter Reflectivities and Standard Deviations.....	10
3	Multipath Results Summary.....	12
4	Theoretical Components of Elevation Tracking Errors Due to Multipath in Snow.....	13
5	Theoretical Total Target Elevation Tracking Errors Due to Multipath in Snow.....	13
6	Signal-to-Clutter Ratios for Several Conditions of Targets and Smoke.....	15
7	Summary of Results (Smoke Week XI).....	20

## ACKNOWLEDGEMENTS

The data that was collected jointly by Rockwell Instrumented Millimeterwave System (RIMS) and CECOM Center for Night Vision and Electro-Optics (C<sup>2</sup>NVEO) personnel during *Smoke Week XI* was under the guidance and supervision of the C<sup>2</sup>NVEO, Visionics Division, Battlefield System Performance Team, and was sponsored under the Assessment of Stationary Target Acquisition Techniques III (ASTAT) Contract No. DAAB07-88-C-F200.

The authors wish to thank RIMS personnel Messrs. Engelke and Ott for collecting data under extreme cold; Dugway Proving Ground and PM SMOKE for providing valuable quantitative multispectral, multipath transmissometer radiometer data; and Messrs. Farmer and Crane of the Science and Technology Corporation, Las Cruces, NM, for helpful discussions on normalizing the transmissometer data relative to smoke concentrations.





## **ROCKWELL INSTRUMENTED MILLIMETER WAVE SYSTEM (RIMS) VAN**

- **TRANSMITTER: 94 GHz, 480 MHz BW, 250 MW PEAK**
- **RANGE SIDELOBES: -27 dB**
- **MONOPULSE ANTENNA: BEAMWIDTH  $\approx$  14 mr, WITH -26 dB SIDELOBES**
- **MULTIPLE POLARIZATION ANTENNA: BEAMWIDTH  $\approx$  14 mr, WITH -26 dB SIDELOBES**

**Figure 1. Data Acquisition System Description**

### **RIMS DESCRIPTION**

The RIMS is a fully instrumented antenna, transceiver, and processor. Two range gates sample data from each transmitted pulse. Sensor characteristics include:

- 94 GHz MMW transmission
  - 250 MW peak (solid state)
  - 480 MHz bandwidth
- Coherent transmit/receive waveforms
- Pulse-to-pulse frequency agility
- Selectable pulse widths (chirp/non-chirp)
- Monopulse and polarization diversity antennas
- Pulse-to-pulse polarization diversity (V, H, LHCP, RHCP)
- Azimuth/elevation beam scan.

Ground truth/radar data correlation include:

- Television (boresighted with radar antenna)
- TV monitor for operator
- Wide field-of-view (FOV) TV camera
- Narrow FOV TV camera (antenna beamwidth size)
- Test site weather stations

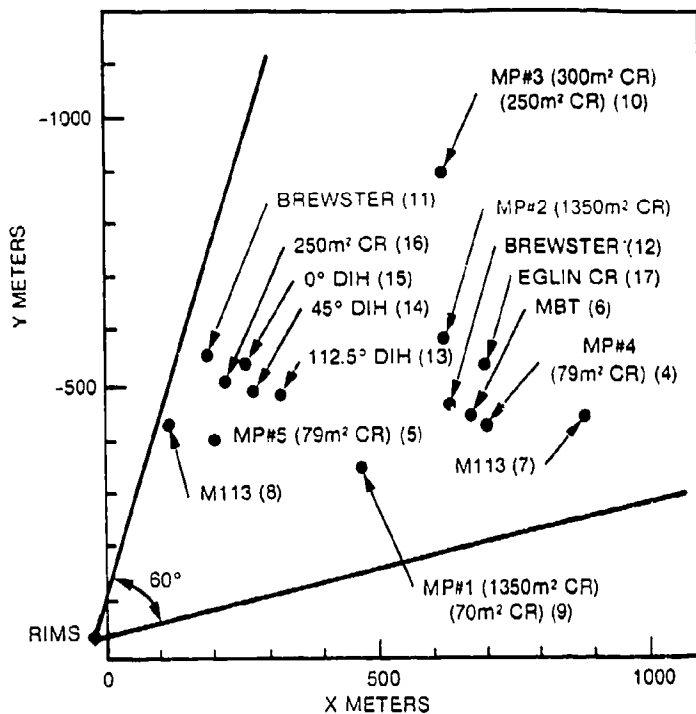
## TEST OBJECTIVES

The specific CECOM Center for Night Vision and Electro-Optics (C<sup>2</sup>NVEO) test objectives during *Smoke Week XI* utilizing RIMS included obtaining:

- Data in order to evaluate attenuation at 94 GHz in different smokes and snowfall rates (polarization diversity and monopulse)
- Cluttermaps of scene as snow and weather environment changes (polarization diversity and monopulse)
- Multipath data at several locations in snow (polarization diversity and monopulse)
- Data on stationary targets for different smoke and snow conditions (polarization diversity and monopulse).

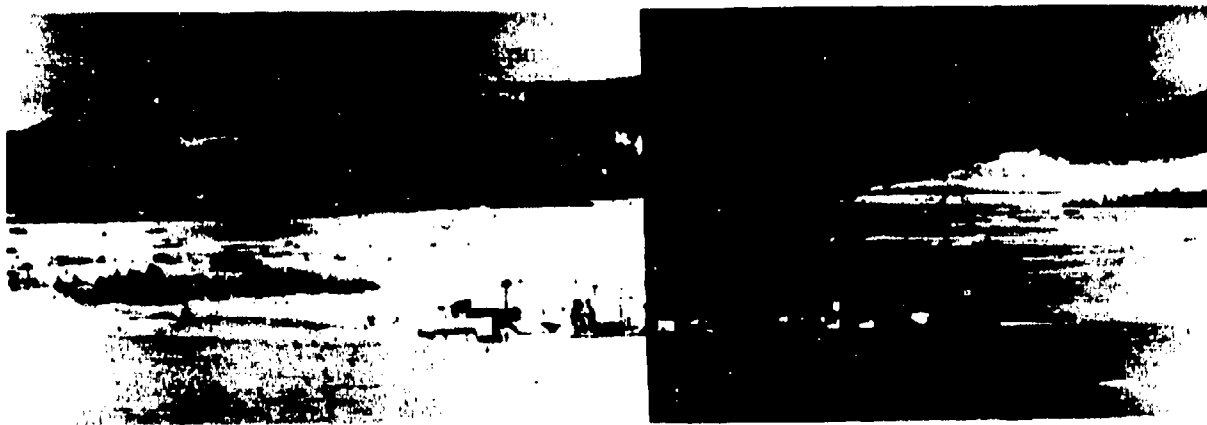
Attenuation tests were conducted against corner reflectors with polarization diversity. Data were taken prior to and during the tests. Cluttermaps, obtained for the scene from 400 to 1,200m over a 60° sector, showed snow backscatter levels for full polarization transmit and receive. In addition, multipath effects were measured in both powdery and metamorphic snow using corner reflectors that were raised and lowered vertically at ranges from 500 to 1,100m. Finally, two fixed targets—a Leopard Tank and an M113 Armored Personnel Carrier (APC)—were imaged with high range resolution polarimetrics on several days as snow and smoke conditions changed.

Figure 2 is a plan view of the test range showing the locations of corner reflectors and targets. Figure 3 is a photograph covering the 60° sector looking out from the radar to where targets and corner reflectors were located and all data were taken.



- Note:**
1. CR - corner reflector
  2. DIH - dihedral
  3. MBT - main battle tank
  4. MP# - multipath site number

**Figure 2. Plan View of Range (Smoke Week XI)**



**Figure 3. Photographs of Test Site**

## SECTION II. TEST DATA

### ATTENUATION IN SNOW

Snow data were taken over several days against dihedrals and corner reflectors using both HH and fully diverse polarizations. The data taken during snowfall were compared to the nearest calibration data to determine attenuation. Snow data was taken on March 2 and 4, 1989. On these days, the snow was falling with various concentrations ranging from  $0.05 \text{ g/m}^3$  to  $0.42 \text{ g/m}^3$ . Measurements were taken at various ranges on these targets and the attenuation was normalized to 1km by multiplying the two-way attenuation measured by the ratio of 1km to the actual range.

The points in Figure 4 show the actual snow concentrations and measured attenuations when normalized to 1km. The particular type of transmit and receive polarizations is indicated by the symbol depicting the data point. Because of the sparsity of the data, a least squares fit was made to all of the polarization data resulting in an estimated two-way attenuation coefficient of  $5.5 \text{ dB/km}/(\text{g/m}^3)$ , as shown in Figure 4.

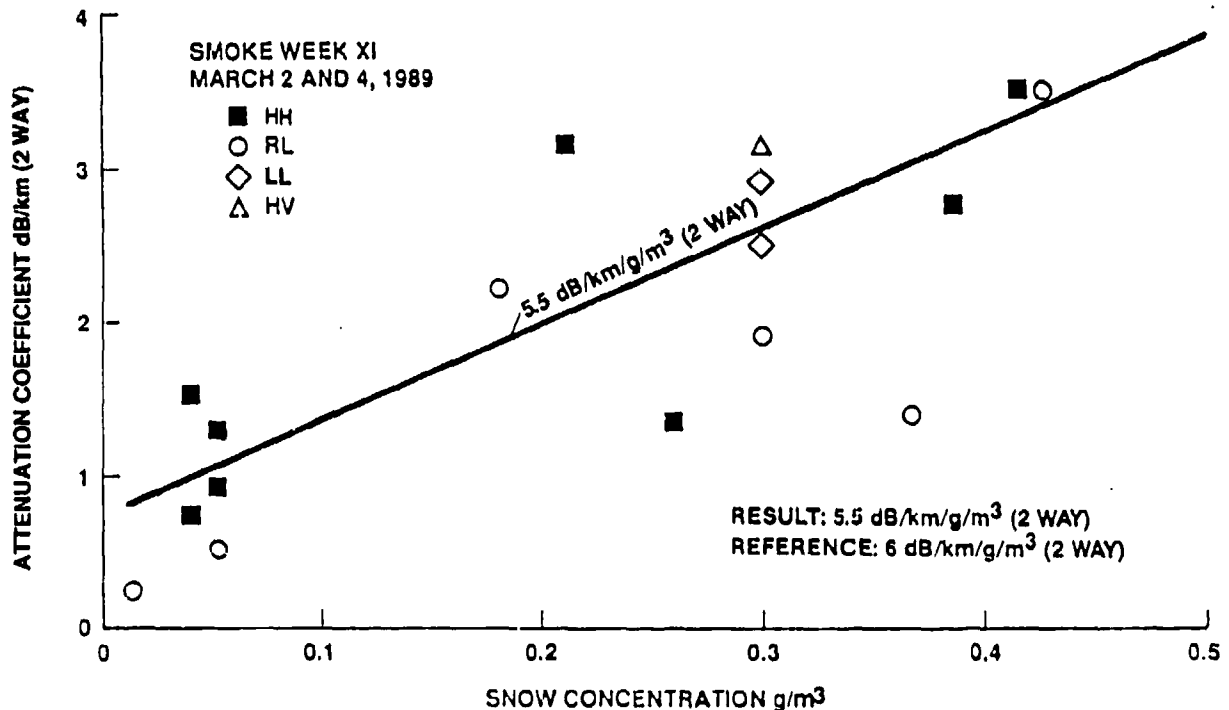


Figure 4. Attenuation in Snow Results

## ATTENUATION IN SMOKE

Attenuation data was taken for several different smokes, as time varied. The attenuation varied sufficiently and rapidly enough to give independent measurements every few seconds as the smoke concentrations in the path length varied. To normalize out these variable path lengths, transmissometer data along the same path as the radar was used to compute a concentration length for each radar measurement. This concentration length allowed the normalization of attenuation data.

The concentration length was obtained in real time from transmissometer measurements at various points in the infrared (IR) spectrum; namely, visible, 1.5 $\mu$ , 3-5 $\mu$ , and 8-12 $\mu$ . From the Beer-Bourguer Law (Ref 2), the one-way transmission is related to the concentration length by the equation:

$$T = e^{-\int_0^L (k) dl} = e^{-\int_0^L (\alpha \cdot \rho) dl} = e^{-\alpha \cdot \int_0^L \rho dl} = e^{-\alpha CL} \quad \text{Equation 1}$$

where T is the transmission, k is the volumetric extinction coefficient, L is the path length,  $\alpha$  is the mass extinction coefficient,  $\rho$  is the concentration (or density), and

$$CL = \int_0^L \rho dl, \quad \text{Equation 2}$$

is concentration length, therefore CL is the integral of concentration over the path length. Given T from measurement, Equation 1 can be solved for CL as

$$CL = -\frac{\ln(T)}{\alpha} \quad \text{Equation 3}$$

if  $\alpha$  is known. For all the smokes tested,  $\alpha$  is known from laboratory experiments and T is known from transmissometer measurements. The concentration length is thus a normalizing constant for transmission paths and was therefore used to quantify radar attenuation. The units were selected as

$$\text{attenuation (two-way) per unit concentration lengths,} \quad \text{Equation 4}$$

or

$$\text{dB (two-way)/(g/m}^2\text{).} \quad \text{Equation 5}$$

To ascertain a concentration length for each radar measurement, a transmissometer was selected that had the same line of sight (or one close to it) as the radar. Each transmissometer had multiple returns at different IR frequencies. The concentration length was computed for each IR frequency, the highest and lowest discarded, and the remainder were averaged to obtain a concentration length for each measurement. Each two-way attenuation measurement was then divided by its corresponding concentration length to obtain the normalized attenuation. For each type of smoke, the normalized attenuation measurements were then used to estimate an attenuation by discarding the highest and lowest measurements and averaging the remainder. If there were less than three measurements, no measurements were discarded. Table 1 gives the resultant estimated attenuations per unit concerning length for the different smokes tested, in the order of increasing attenuation.

From Table 1, the median two-way attenuation per concentration length is 0.25 dB/g/m<sup>2</sup> (white phosphorus) with a peak two-way attenuation for brass smoke of 1.09 dB/g/m<sup>2</sup>. Reference 1 gives more details of the specific test data. The appendix gives typical concentration lengths for heavy, moderate, and light smoke.

**Table 1. Estimated (Two-Way) Attenuation in Smoke Per Unit Concentration Length**

TYPE OF OBSCURANT	2-WAY ATTENUATION/CL (dB/g/m <sup>2</sup> )	NUMBER OF DATA POINTS	STANDARD DEVIATION
Kaolin/Silica	0.02	1	—
Red Phosphorus	0.09	2	0.06
JP8	0.12	4	0.01
Kaolin/Fog Oil	0.22	1	—
White Phosphorus (WP)	0.25	4	0.03
Aluminum	0.64	6	0.40
Graphite	0.70	3	0.27
Fog Oil	0.78	1	—
Brass	1.09	5	0.70
Median (WP)	0.25	—	—
Worst Case (Brass)	1.09	—	—

## SNOW BACKSCATTER

Several cluttermaps were made of the test area. A cluttermap is a map of the RCS returned over a search area as the radar is scanned in range, elevation, and azimuth. Figures 5 and 6 are two examples of cluttermaps taken at near and far ranges covering the entire test area. In these maps, each resolution cell is 6m long in range and 0.5° in azimuth. The depicted amplitude is the non-coherent sum of the returns from 1,440 pulses at three elevations, 480 pulses at each elevation (10 pulses at each frequency over 48 frequencies spaced 10 Mhz apart for a total bandwidth of 480 MHz). The amplitude was then calibrated based on the return from known magnitude corner reflectors in the scene. Thus, the figures depict a three-dimensional picture where azimuth and range are the planar coordinates and amplitude in dB m<sup>2</sup> is the height coordinate. These figures show the large amount of clutter in the scene, primarily due to instruments, targets, and radar reflectors placed in the scene during the conduct of the test.

By selecting areas in the cluttermaps that had no targets in them, measurements of 94 GHz MMW backscatter in snow were obtained. The average measured returns at different ranges were plotted and the least square curve fit to the data. Results for Site 2 are plotted in Figure 7, page 10. Note that these results are different than the preliminary study in Ref 1, since an error in data reduction was discovered since Reference 1 was published.

By using the formula,

$$\text{RCS} = \sigma_0 R (\theta) (\Delta R) \quad \text{Equation 6}$$

where RCS is the returned signal strength,  $\sigma_0$  is the clutter reflectivity coefficient, R is the range,  $\theta$  is the beamwidth (0.133 rad.), and  $\Delta R$  is the range resolution,  $\sigma_0$  was computed as -37 dB, -36 dB, and -35 dB at Sites 1, 2, and 4, respectively.

At Site 3, a fully polarimetric cluttermap was taken and a  $\sigma_0$  computed on a 0.0045 km<sup>2</sup> area devoid of corner reflectors for RR, LL, LR, HH, VV, and HV polarization pairs on March 1, 1989. The resultant  $\sigma_0$ 's and standard deviations are given in Table 2, page 10.

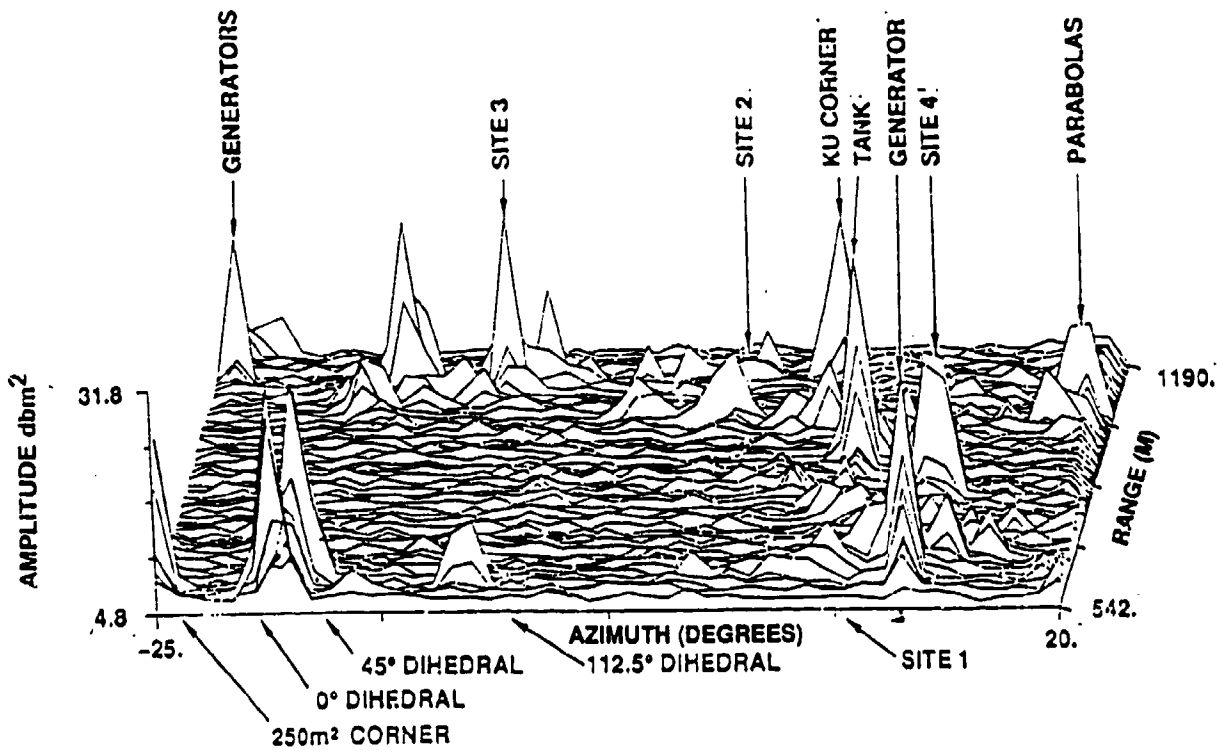


Figure 5. Cluttermap of Test Area (500-1,200m), HH Polarization, 3/4/89

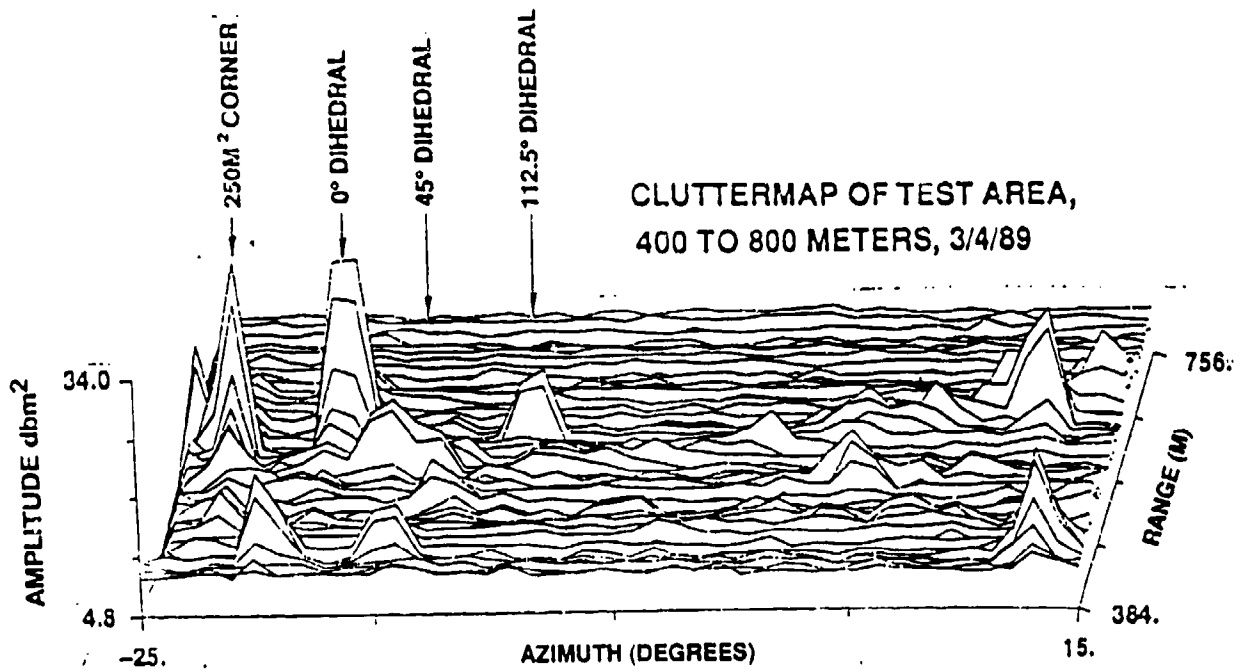


Figure 6. Cluttermap of Test Area, HH Polarization

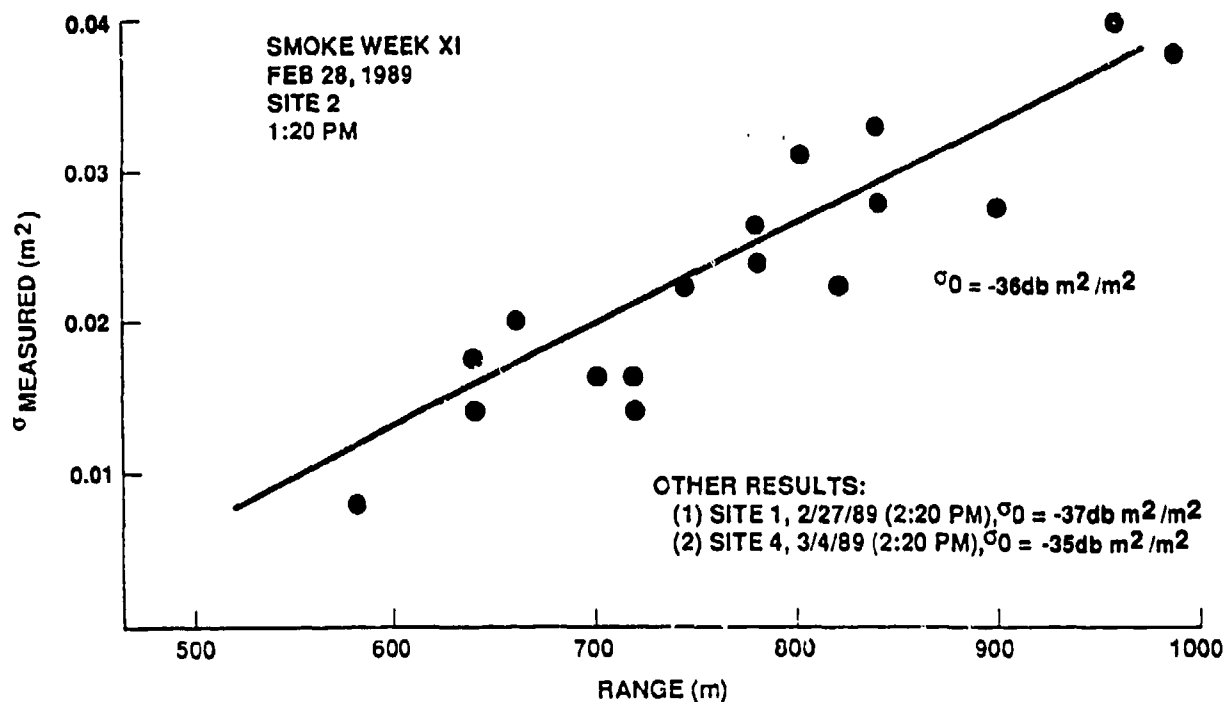


Figure 7. Snow Backscatter Results, HH Polarization

Table 2. Polarimetric Clutter Reflectivities and Standard Deviations

POLARIZATION PAIR	REFLECTIVITY ( $dB m^2/m^2$ )	STANDARD DEVIATIONS (dB)
RR	-32.7	1.5
LL	-33.1	1.3
LR	-35.7	1.3
VV	-36.1	1.2
HH	-36.4	1.4
HV	-33.1	1.4

\* Site 3 (3/1/89), open field, powdery snow

## MULTIPATH MEASUREMENTS

These tests were conducted by raising and lowering corner reflectors on a stand and reading RCS at each position of the corner reflectors.

The data were mostly diffuse multipath since the periodicity was variable although some specular multipath was observed. Using the equation

$$\sigma^2 [\delta^2 + 1] + 2\delta \cos(\phi) = \text{RCS}, \quad \text{Equation 7}$$

the RCS variations were modeled as  $\phi$  varies. The variable  $\phi$  is linear if specular and random if diffuse. To obtain the specular and diffuse multipath components, a regression was made to determine periodic and random components to the RCS variation as well as the mean level. Figure 8 gives a typical sample.  $\delta$  is the multipath reflection coefficient.

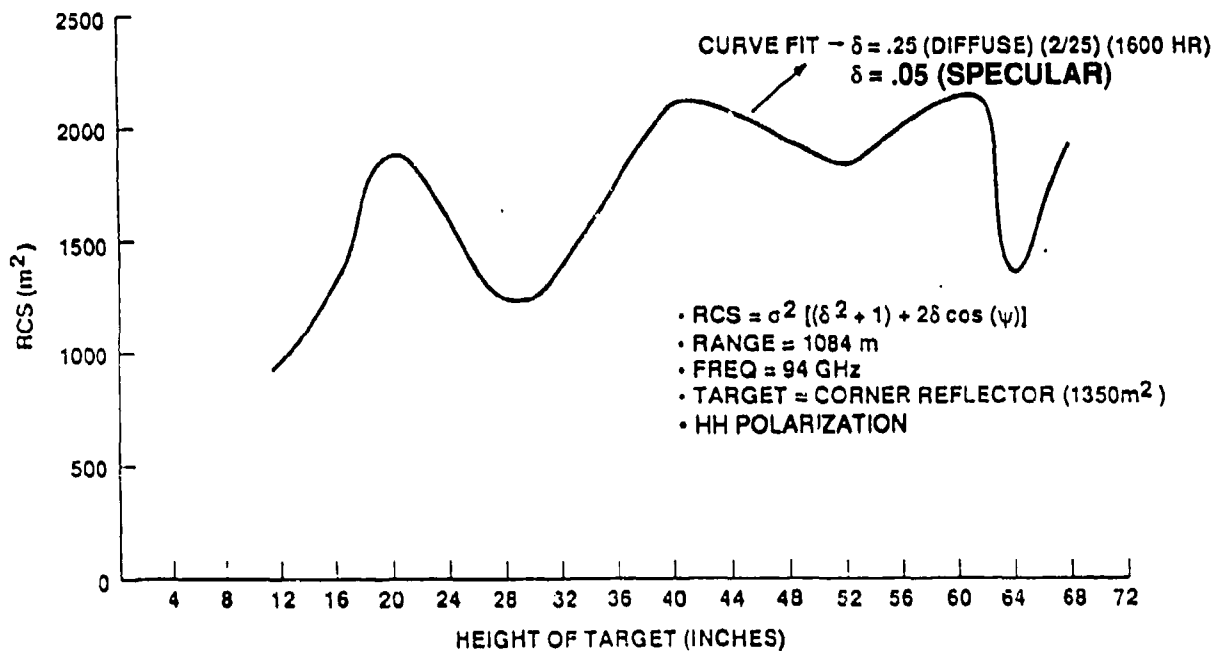


Figure 8. Multipath in Snow Results

The multipath effect is a reflection of the electromagnetic radiation from the ground or other objects between the transmitter and target. Multipath causes two effects: (1) loss of augmentation of received signal due to destructive or constructive interference between the direct and indirect radiation, and (2) movement of the tracking point in elevation and/or azimuth dependent on the direction of the multipath radiation. In this study, effect (1) was used to estimate the multipath reflection coefficient, the specular part due to reflection from a smooth plane, and the diffuse part due to multiple nonplanar surfaces. Table 3 summarizes all multipath coefficients obtained at *Smoke Week XI*. Both specular and diffuse coefficients were obtained.

**Table 3. Multipath Result Summary**

DATE	CORNER	CLUTTER CONDITION	SITE	RANGE (m)	$\rho$ DIFFUSE	$\rho$ SPECULAR	POLARIZATION
	REFLECTOR						
2/23		Powdery Snow (Few Tracks)	1	547	0.25	0.05	HH
2/24		Powdery Snow	1	587	0.25	0.05	HH
2/24		Powdery Snow	2	858	0.33	0.35	HH
2/25		Powdery Snow (Some Tracks) (See Figure 19)	3	1,084	0.25	0.05	HH
3/5 (1418)		Powdery Snow (Many Tracks)	4	829	0.32	0.15	HH
3/5 (1355)		Powdery Snow (Many Tracks)	4	829	0.3	0.16	HH
3/9		Metamorphic Snow	4	829	0.44	0.4	HH
3/9		Metamorphic Snow	5	418	0.37	0.4	HH
Average		Powdery Snow		—	0.28	0.14	HH
Average		Metamorphic Snow		—	0.41	0.4	HH

In Ref 3, a theory is developed which breaks the multipath into the two parts and, in Ref 4, a statistical multipath error model is developed for those parts. For an extended target on the surface, such as a tank or APC, this reference shows that the multipath error is a function of target height and reflection coefficient and has a bias and random part at a single frequency. The random part is dependent on frequency and can be reduced by averaging over broad bandwidth, independent measurements for a tank or APC being obtained at about 40 MHz intervals.

For a uniformly distributed target of 2m height, the above theory shows that the multipath tracking error for RIMS will be independent of range and is given in Table 4. The bias errors will be biased downward and can be compensated if the reflection coefficient and target height are known. The random error, can be reduced by wider bandwidth.

The total theoretical tracking error, due to both specular and diffuse multipath, is given in Table 5.

**Table 4. Theoretical Components of Elevation Tracking Errors Due to Multipath in Snow**

(Reflection Coefficient = 0.35; target is a tank or APC of 2m height; RIMS (i.e., 480 MHz bandwidth); target is uniformly distributed in height.)

CONDITION	TRACKING ERROR DUE TO SPECULAR MULTIPATH		TRACKING ERROR DUE TO DIFFUSE MULTIPATH	
	Random	Bias	Random	Bias
Powdery Snow	0.21m	0.12m	0.24m	0.16m
Metamorphic Snow	0.27m	0.4m	0.28m	0.3m

**Table 5. Theoretical Total Target Elevation Tracking Errors Due to Multipath in Snow**

(RIMS; target height = 2m)

CONDITION	TOTAL TRACKING ERROR	
	Random	Bias
Powdery Snow	0.32m	0.28m
Metamorphic Snow	0.39m	0.7m

## SECTION III. SNOW AND SMOKE EFFECTS ON TARGETS

During the data collection, a Leopard Tank was placed in the target area and data were collected in various snow levels and smoke. Since the RIMS system has 480 MHz bandwidth, approximately 1-foot resolution high range profiles of the targets can be generated. Some of these were generated and are plotted in Figure 9. The plots show that the range profile is most severely distorted by snow up to 5 or 10 dB and internal features somewhat distorted by smoke.

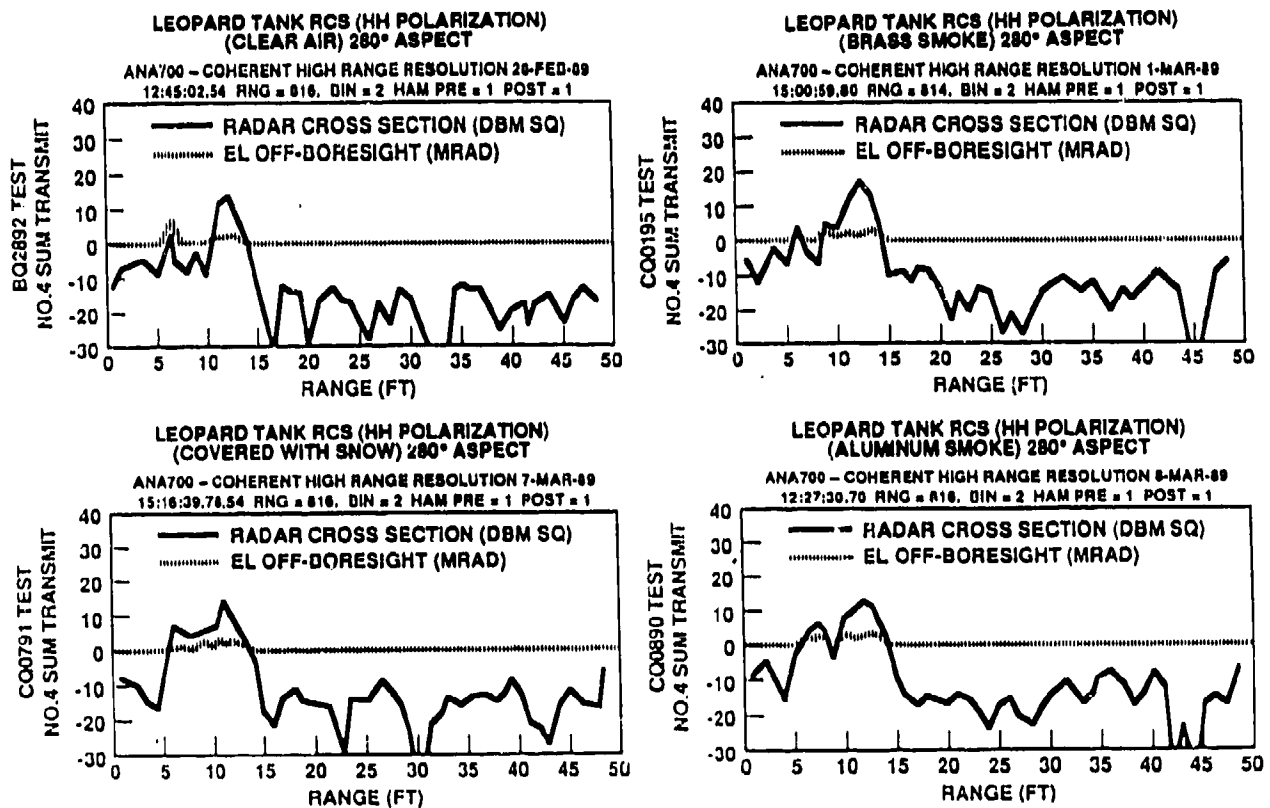


**Figure 9. Effect of Smoke and Snow on Range Profiles**

Assuming log normal distributed targets and clutter with standard deviations given in Table 2, a target standard deviation of 6 dB and no CFAR loss, Figure 10 gives the expected performance. The curves show the VH polarization gives the poorest performance but is relatively insensitive to clutter. Overall, HH polarization gives the most consistent performance on both targets with essentially no degradation in smoke. RR and LL polarization also show a low sensitivity to the smokes with LL being slightly stronger on the M113 APC. VV polarization seems to be very sensitive to aluminum and brass smoke but gives strongest results on the M113 APC. RL polarization demonstrates a sensitivity to brass smoke. The other variations in Table 6 are probably due to receiver gain variations and experimental noise.

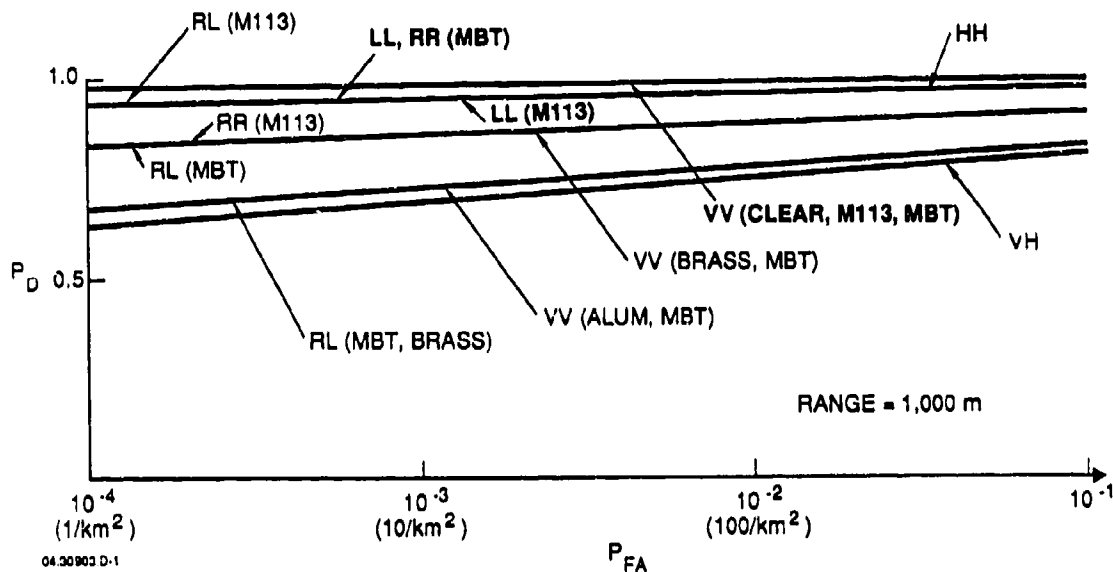


Figure 10. Expected Target Detection Performance in Clutter as Polarization Varies (False alarms per  $\text{km}^2$  are for RIMS at 1 km.)

Table 6. Signal-to-Clutter Ratios for Several Conditions of Targets and Smoke

TARGET CONDITION	RR	RL	LL	VV	VH	HH
MBT (Snow and Brass/Oil)	11.4	7.65	13.9	11.1	4.8	14.8
MBT (Aluminum)	13.4	10.65	13.8	7.1	6.8	16.8
MBT (Clear)	13.9	11.4	12.3	15.1	5.8	13.8
M113 (Graphite)	11.4	16.9	16.3	19.6	7.3	16.3
M113 (Clear)	8.9	15.65	15.3	18.6	5.8	14.3

Polarimetric data was taken on a MBT (Leopard) and on an M113 APC. The polarization of RR, RL, LL, VV, VH, and HH were collected and compared. The signal-to-clutter ratio was computed at 1,000m and is compared in Table 6 for the various polarizations where the clutter reflectivity and standard deviation are given in Table 2. From this data, a selection can be made for the polarization that gives the best detection performance in clutter.

Figures 11 through 15 give the variations of the target high range resolution signature as polarization, target, and smoke vary. The profiles are cyclic with 48 foot ambiguity intervals. The copol return has the nearest range at the right of the figures and the crosspol return has nearest range on the left of the figures. Therefore, the copol and crosspol returns do not line up in range except at the ambiguity points (0 or 48 foot). The targets are between 10 and 30 feet long and give a return much stronger than the clutter. The clutter is about -15 to -20 dB m<sup>2</sup> or less. It is clear from these figures that the snow clutter (i.e., the surrounding snow) gives a stronger return for the RR, LL, and VV polarization than the RL, HV or HH polarizations. The aspect angle of 0° is the target frontal aspect and is measured counterclockwise.

Figures 11 through 15 also show that the MBT (Leopard) profile is only slightly modified as the aluminum and brass smoke are added for RR, LL, and HV polarizations, but more significant changes are made to the HH, VV, and RL polarization profiles. For the M113 APC, no polarization seems to have a significant profile change with graphite smoke. Therefore, the metalized smokes apparently have significant effect on odd-bounce scatter profiles such as HH, VV, and RL, but little effect on even-bounce scatter profiles such as dihedral sensitive polarizations (i.e., HV, RR, and LL). There was little effect on profiles or RCS due to graphite smoke at all polarizations.

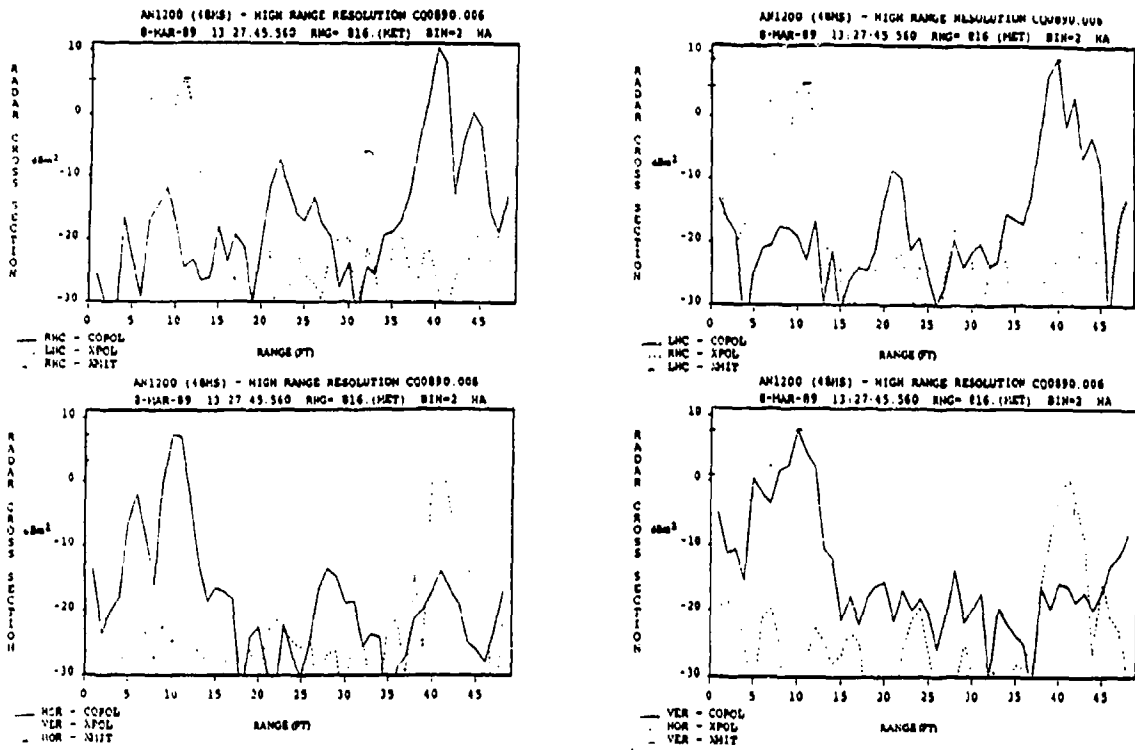


Figure 11. Leopard Tank, Clear, 280° Aspect

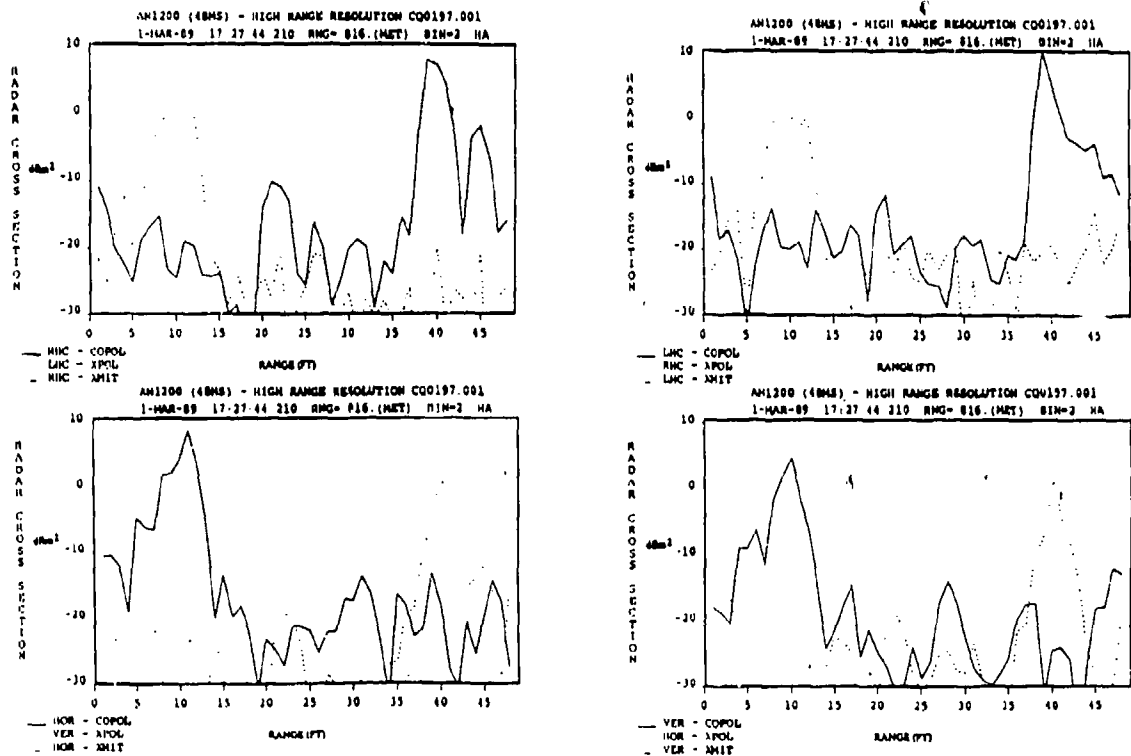


Figure 12. Leopard Tank, Falling Snow Plus Brass/Fog Oil Smoke, 280° Aspect

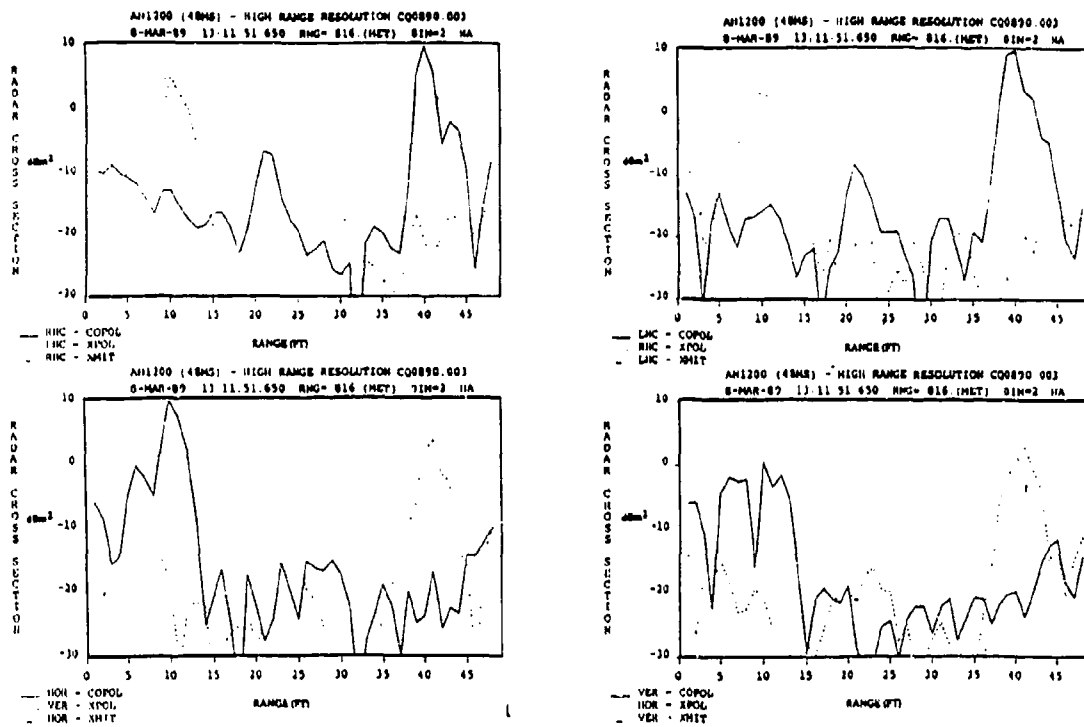


Figure 13. Leopard Tank with Aluminum Smoke, 280° Aspect

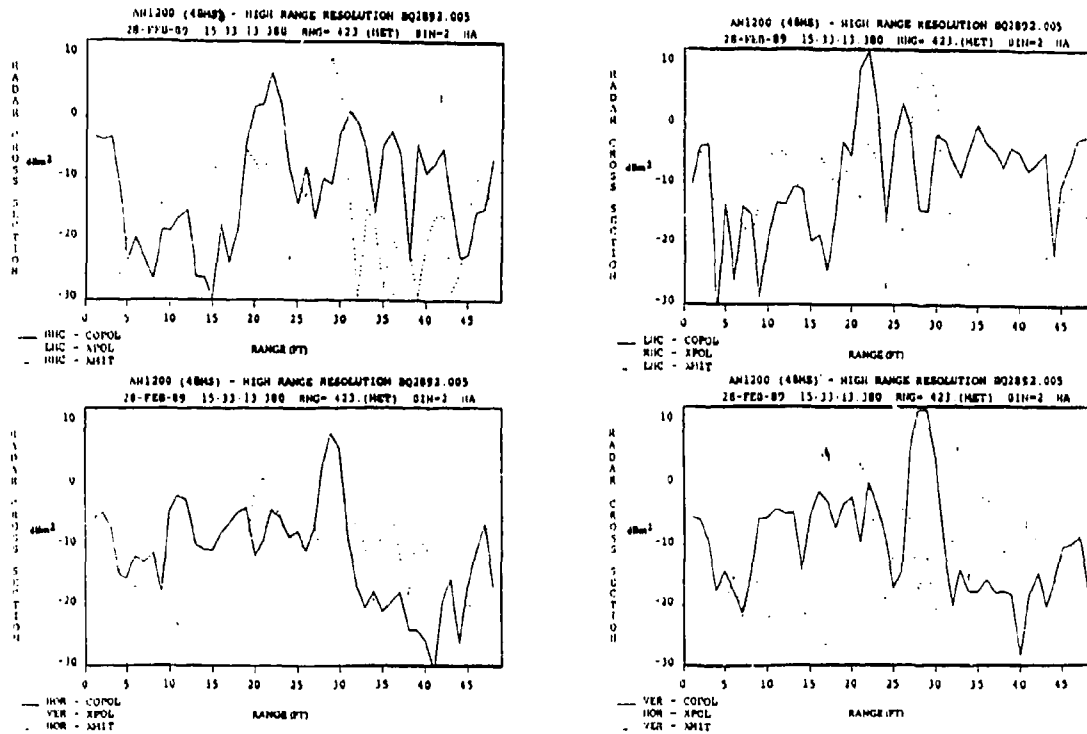


Figure 14. M113 APC, Clear, 0° Aspect

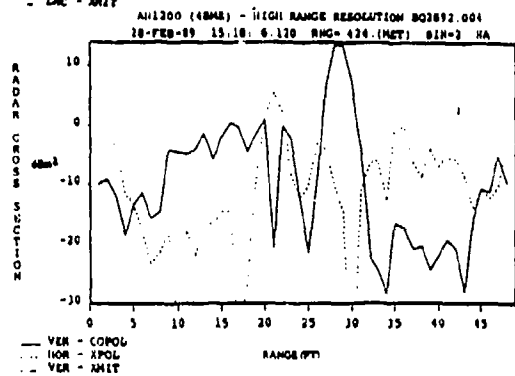
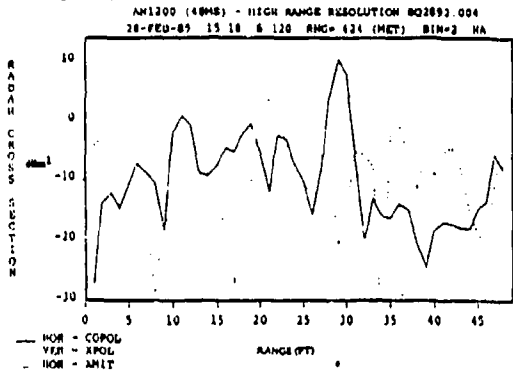
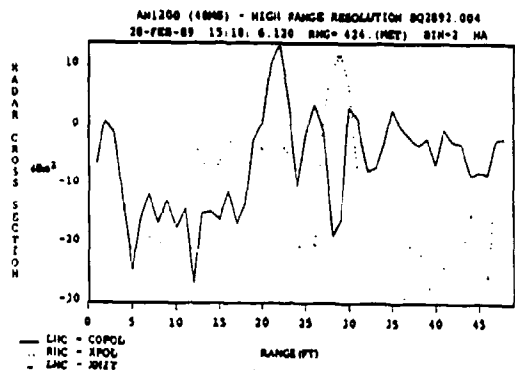
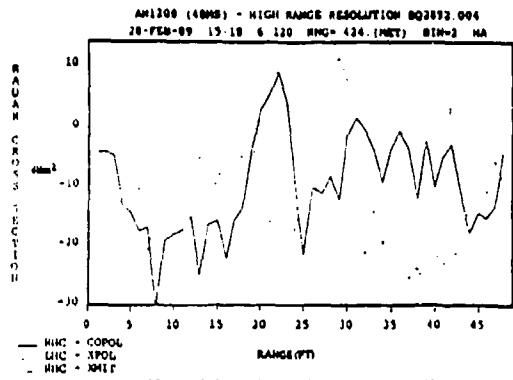


Figure 15. M113 APC with Graphite Smoke, 0° Aspect

## SECTION IV. SUMMARY

Table 7 summarizes the results of the data taken at *Smoke Week XI*. The results compare well to the available reference on snow. No reference could be found on snow backscatter at 0° grazing. Expected performance with the multipath reflection coefficients obtained is given in the report (Table 5) as well as the expected detection performance with different polarizations in smoke (Figure 10). The even-bounce polarizations appear to have an advantage over odd-bounce polarization combinations in metalized smoke because of less profile variations.

**Table 7. Summary of Results (Smoke Week XI)**

DESCRIPTION OF PARAMETER	MEASURED RESULTS	OTHER SOURCE RESULTS
Attenuation in Snow	5.5 dB/km/(g/m <sup>3</sup> ) (2-way)	(Ref 5) 6 dB/km/(g/m <sup>3</sup> ) (2-way)
Attenuation in Smoke		
Median (White Phosphorus)	0.25 dB/(g/m <sup>2</sup> ) (2-way)	—
Worst Case (Brass)	1.09 dB/(g/m <sup>2</sup> ) (2-way)	—
Snow Backscatter (0° Grazing) (Site 3)		
All Polarizations	-33.1 to -36.4 dB	(Ref 6) (-10 to -17 dB) at 10° grazing
Multipath Reflection Coefficient		
Powdery Snow	Specular = 0.14 Diffuse = 0.28	— —
Metamorphic Snow	Specular = 0.4 Diffuse = 0.41	— —
Target RCS Mods in Snow	5 to 10 dB RCS chances	—
Target RCS Mods in Smoke		
Graphite Smoke	Minor for all polarizations	—
Metalized Smoke	Minor for RR, LL, HV Significant for HH, VV, RL	—

## REFERENCES

1. *Smoke and Snow Effects on 94 GHz Sensors (Preliminary Results)*, Williams and Matsumoto, Smoke/Obscurants Symposium XIII; April 25-27, 1989.
2. *Smoke and Natural Aerosol Parameters (SNAP) Manual*, Smoke and Aerosol Working Group, Publications No. 61-JTCG/ME-85-2, Oklahoma City ALC, ATTN: MMEDUD, Tinker AFB, OK 73145-5979; April 26, 1985.
3. *The Scattering of Electro Magnetic Waves from Rough Surfaces*, Beckmann and Spizzichino; 1963.
4. *Statistical Theory of Extended Radar Targets*, Ostrovityanov and Basalov; 1985.
5. *Snow Field Tests*, Nemarich; 1981.
6. *Principles and Applications of MMW Radar*, Currie and Brown; 1986.

**APPENDIX**  
**TYPICAL SMOKE CONCENTRATION LENGTHS (g/m<sup>2</sup>)**

<b>TYPE OF SMOKE</b>	<b>HEAVY SMOKE</b>	<b>MODERATE SMOKE</b>	<b>LIGHT SMOKE</b>
Kaolin/Silica	2.4	1.2	0.4
Red Phosphorus	0.8	0.4	0.1
JP8	0.5	0.2	0.1
Kaolin/Fog Oil	1.0	0.5	0.2
White Phosphorus	0.8	0.4	0.1
Aluminum	2.5	1.3	0.4
Graphite	0.7	0.4	0.1
Fog Oil	0.4	0.2	0.1
Brass	2.7	1.4	0.4
Assumed Optical Depth	3.0	1.5	0.5

## DISTRIBUTION FOR REPORT NO. AMSEL-RD-NV-0090

2	Defense Technical Information Center ATTN: DTIC Cameron Station Alexandria, VA 22304-9990	1	Director US Army CECOM, Center for Night Vision & Electro-Optics
		6	ATTN: AMSEL-RD-NV-V Fort Belvoir, VA 22060-5677
1	HQDA ATTN: DACA-CA Washington, DC 20310	1	Product Manager-REMBASS US Army Communications-Electronics Command Fort Monmouth, NJ 07703-5001
1	Deputy Undersecretary of the Army Research and Development HQDA, The Pentagon Washington, DC 20310	1	Commander US Army Concepts Analysis Agency 8120 Woodmont Avenue Bethesda, MD 21004
1	Commander Harry Diamond Laboratory ATTN: DELHD-AC 2800 Powder Mill Road Adelphi, MD 20783-1145	1	Program Executive Officer US Army Intelligence and Electronic Warfare Center ATTN: AMCPEO-IEW Vint Hill Farms Station, Bldg 209 Warrenton, VA 22186-5115
1	Commander US Army Aviation Applied Technology Directorate ATTN: SAVRT-TY-MSS Fort Eustis, VA 23604-5577	1	Commander US Army Laboratory Command ATTN: AMSEL-C 2800 Powder Mill Road Adelphi, MD 20783-1145
1	Project Manager Army Helicopter Improvement Program US Army Aviation Systems Command 4300 Goodfellow Boulevard St. Louis, MO 63120-1798	1	Commander US Army Materiel Command ATTN: AMC-PA Alexandria, VA 22333-0001
1	Program Manager Light Helicopter Family US Army Aviation Systems Command 4300 Goodfellow Boulevard St. Louis, MO 63120-1798	1	Director US Army Signal Warfare Center ATTN: AMSEL-RD-SWC Vint Hill Farms Station Warrenton, VA 22186-5013
1	Project Manager Target Acquisition Designation System/ Pilot Night Vision System (TADS/PNVS) US Army Aviation Systems Command Bldg 105 4300 Goodfellow Boulevard St. Louis, MO 63120-1798	1	Project Manager US Army Tactical Mgmt Info Systems Building T-601 Fort Belvoir, VA 22060-5456
1	Product Manager UH-1 Aircraft US Army Aviation Systems Command ATTN: AMCPEO-CCS 4300 Goodfellow Boulevard Ft. Monmouth, NJ 07703-5000	1	Office of the Undersecretary of Defense Research and Engineering Tactical Warfare Programs, Land Warfare ATTN: OUSDRE-TWP The Pentagon Washington, DC 20301

Distribution-1